Cost-effective n-Pasha solar cells with efficiency above 20%

Ingrid Romijn, **Astrid Gutjahr**, **Desislava Saynova**, **John Anker**, **Eric Kossen** & **Kees Tool**, ECN Solar Energy, Petten, The Netherlands

ABSTRACT

This paper presents recent developments of ECN's n-Pasha (passivated on all sides H-pattern) solar cell technology. The n-Pasha cell, currently being produced on an industrial scale by Yingli Solar, is a solar cell fabricated on n-type Cz material with homogeneous diffusions, dielectric passivation and printed metallization on both sides. The metallization is applied in an open H-pattern to both sides, which makes it suitable for bifacial applications. In order to improve both cell performance and the cost of ownership of n-Pasha solar cells, the ECN R&D team has focused on several aspects of the device design and processing. By reducing metal coverage and improving the quality of the front-side metallization, tuning the back-surface field (BSF) doping and improving the front- and rear-surface passivation, it has been possible to obtain an average efficiency of 20%, with top efficiencies of 20.2%. At the same time, the amount of silver used for metallization has been decreased by over 50% and is now similar to that used for p-type solar cells. Furthermore, it is shown that with the ECN n-Pasha cell concept, wafers from the full resistivity range of n-Cz ingots can be used to make cells without losses in efficiency. Combining the improved efficiency and the reduction in cost makes the n-Pasha cell concept a very cost-effective solution for manufacturing highly efficient solar cells and modules.

Industrial solar cells and modules on n-type base material

The fourth edition of the International Technology Roadmap for Photovoltaics [1] predicts a clear shift from p-type to n-type mono-Si within the mono-Si market. The market share for n-type mono will be equal to that of p-type mono in 2017, and will exceed it the following years. Compared with p-type material, n-type Cz material is known for its stable high carrier lifetimes because of the absence of light-induced degradation (LID) [2,3] and its higher tolerance of the most common metallic impurities, such as Fe [4,5]. These longer lifetimes are consequently reflected in higher efficiencies. Indeed, the highest-efficiency crystalline silicon modules currently on the market are based on SunPower Maxeon technology [6], which incorporates n-type Cz material. Using this technology, SunPower fabricates interdigitated back contact (IBC) solar cells with efficiencies of over 24%, which enables module efficiencies of up to 21% to be achieved [7]. IBC solar cells feature both the emitter and the back-surface field (BSF) at the rear of the solar cell. Metal contacts are formed solely on the rear, which means that the complete front surface is available for capturing the light. Since the p-n junction is located at the rear of the cell, the IBC cell must be fabricated on Si wafers with a long effective minority-carrier diffusion length in order that all the carriers reach the emitter. Excellent front-surface passivation is therefore required as well. The production cost of these high-efficiency cells is quite high owing to the use of many complicated processing steps [8]. Using its heterojunction with intrinsic thin layer (HIT) technique, Sanyo Electric Corporation has obtained very high efficiencies with n-Cz material as well: efficiencies above 23% were reported in 2009 [9], and recently these efficiencies have improved even further [10]. In this case, the high-efficiency processing also leads to higher production costs than for standard (p-type) solar cells [8].

> "The n-Pasha cell structure itself is simple, while still enabling cell efficiencies above 20%."

ECN's aim is to develop high-efficiency, low-cost and robust solar cell and module concepts that can be easily adopted by industry. One of ECN's cell concepts using n-type silicon is the n-Pasha (passivated on all sides H-pattern) solar cell concept [11]. Compared with the established n-type solar cell techniques described above, the n-Pasha cell concept can be implemented using processing steps that are similar to those found in the production of common p-type solar cells. The n-Pasha cell structure itself is simple, while still enabling cell efficiencies above 20%. This novel cell concept was first introduced to the market in 2010 under the brand name Panda [12,13] by the company Yingli Solar in collaboration with Tempress BV and ECN. Efficiencies of over 19% were reached in 2011 with this cell concept, both by Yingli and by ECN. In 2012 ECN reported efficiencies of up to 20%, obtained by the implementation of improved processing that is currently also being carried out at Yingli [13,14,15]. Furthermore, Yingli demonstrated that their Panda cells show no LID and have a lower temperature coefficient than standard p-type solar cells [13].

Despite the obvious advantages of n-type base material in terms of longer bulk carrier lifetime and subsequent higher efficiencies and an absence of LID, the majority of industrial solar cell and module manufacturers are still using p-type mono- or multicrystalline silicon as their base material. One reason for this is the n-type Cz base material itself: because of the higher segregation coefficient of phosphorus compared with boron, the resistivity range of phosphorus-doped n-type ingots is typically wider than that of boron-doped p-type material. This larger range poses additional challenges for the cell architecture for n-type solar cells, or increases the cost of the solar cells as a result of yield loss if only part of the resistivity range can be used [16]. The second reason is that the cost of n-type cell production is higher than for p-type cell processing. For most concepts, including the n-Pasha cell concept, an additional BBr_3 diffusion step to form a boron emitter is necessary. More importantly, the silver consumption is higher for n-type cells. Because of the absence of the (cheap) aluminium on the rear side, both the emitter and the BSF have to be contacted by a silver grid. However, the costs of printing a full-area layer of aluminium on the back side, which today are still significant, are of course absent for the n-Pasha cell concept.

Recent developments at ECN to lower the cost per watt (€/Wp) of the n-Pasha cell concept are discussed in this paper. In the first part, the n-Pasha cell concept and the steps that were taken to increase efficiency are summarized. In the second and third parts, two main factors having a bearing on the costs of n-type solar cells are described, namely the n-type Cz material

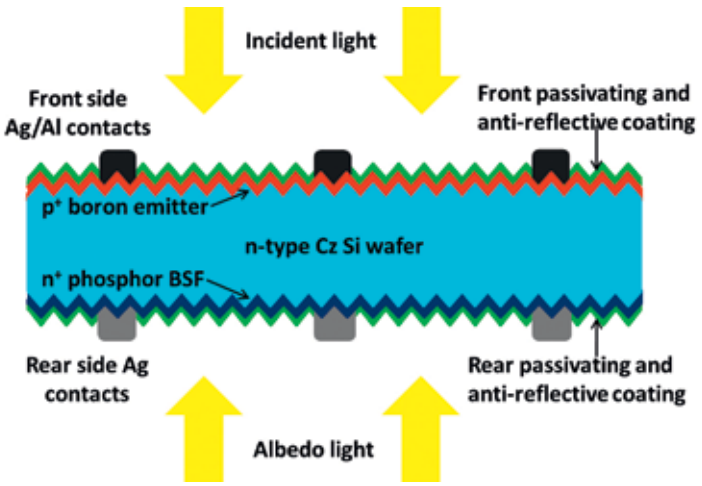

Figure 1. Cross section of the ECN n-Pasha cell, featuring an n-type Cz Si wafer with a boron p^+ emitter and a phosphorus n^+ BSF. Yingli's Panda cells are also based on this structure.

itself and the silver consumption. Measures that can be taken to lower the costs are illustrated. It is shown that the efficiency of n-Pasha solar cells is high and stable over a wide resistivity range, and that the costs relating to the silver metallization can be significantly reduced while maintaining, or even increasing, the solar cell efficiency. The combination of the improved efficiency and the cost reduction makes the n-Pasha cell concept a cost-effective solution for manufacturing highly efficient solar cells and modules.

ECN's n-Pasha cell concept

The basic configuration of the n-Pasha solar cell is shown in Fig. 1. At ECN, the n-Pasha cells are fabricated on 6-inch n-type Cz Si wafers. All the processing steps used for the n-Pasha cell are suitable for industrial-scale implementation. The first processing step is the texturing of the wafers with random pyramids using alkaline etching. The boron emitter and phosphorus BSF are formed using an industrial tube furnace from Tempress [17]. A 60Ω/sq emitter is made using BBr_3 as the precursor. The BSF is created using $POCl_3$ as the precursor and provides additional lateral conductivity on the rear side. This results in a satisfactory fill factor despite the open rear-side metallization, even for cells processed on high-resistivity base material (~10Ωcm). Consequently, the BSF is an important element of the cell design, providing a solution for reducing the performance sensitivity to variations in n-type wafer resistivity. Both the front and rear sides are coated with SiN_x layers for passivation and anti-reflective purposes. The metal grids are then printed, and the contacts on the emitter and the BSF are formed during a single co-firing step. Direct soldering to both the front and rear metallization is possible, so no additional metallization step is necessary to enable interconnection in creating a module.

The open front- and rear-side metallization ensures that the bowing of the cells will be considerably reduced when (very) thin wafers are used, which is a distinct advantage in view of the bowing that occurs with full aluminium BSFs on p-type solar cells. Furthermore, the dielectric coating on the rear side results in an improved surface passivation compared with the conventional full aluminium rear side of a p-type cell, while the optical properties of the dielectric layer can be tuned to achieve optimal (anti-) reflective properties. If the cells are arranged in a standard monofacial module, the refractive indices can be tuned to obtain maximum reflection in combination with the module back-sheet foil. On the other hand, the open rear-side H-patterned metallization makes the n-Pasha concept highly suitable for bifacial cell and module technology. In this way, an even higher module output power and an increased annual energy yield can be realized when the cells are appropriately placed in the field. Recent results have shown that the output power of bifacial n-Pasha modules can be increased by almost 20% if the bifacial modules are placed in front of a reflecting surface [14].

> "The open rear-side H-patterned metallization makes the n-Pasha concept highly suitable for bifacial cell and module technology."

Efficiency improvements of n-Pasha

The processing improvements that have led to the achievement of 20% efficiency of n-Pasha cells have already been described in several publications in 2012 [14,15]. In this section, a brief summary of these steps will be given and the latest results presented.

Front-side metallization

Besides being one of the major cost drivers of solar cells, the front metallization is also a very important parameter of n-Pasha cell efficiency. When the metal-covered area is decreased, the short-circuit current (I_{sc}) and the open-circuit voltage (V_{oc}) will

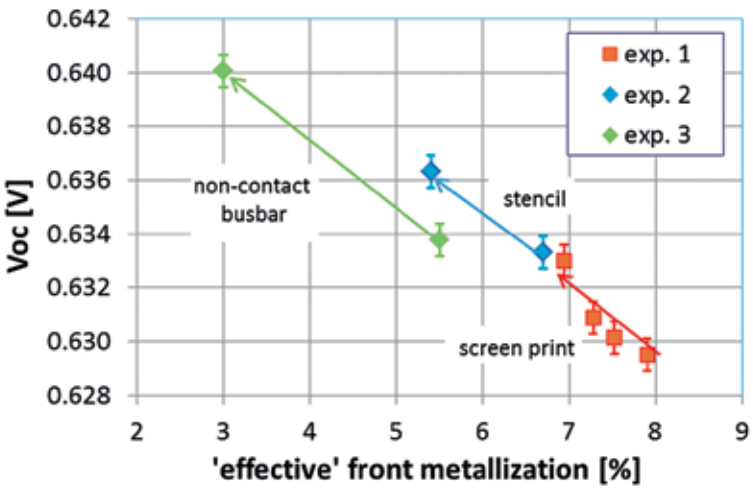

Figure 2. The gain in V_{oc} as a result of improved metallization. The total metallized area is gradually reduced by 2.5% in experiments 1 and 2, resulting in an increase in V_{oc} of 6mV. The reduced recombination under the 2.5% area covered by non-contacting busbars in experiment 3 (performed on a different material) also resulted in an increase in V_{oc} of 6mV, for an 'effective' front metallization of only 3%.

increase as a result of reduced shading losses and reduced recombination below the metal area [18,19]. The challenge is to keep the resistive losses at a minimum and thus maintain a high fill factor (*FF*).

Recent improvements in the front-side metallization of n-Pasha cells can be summarized in the following three steps, each tested via three different experiments and illustrated in Fig. 2; for each experiment, groups of approximately 20 cells were processed. In the first experiment (red squares) the line width of the screen-printed fingers was reduced from 125µm to 100µm, while in the second experiment (blue diamonds) the line-width was reduced even further, to 60µm, by using stencil printing of the fingers instead of screen printing. The advantages of stencil printing for front-side metallization of n-Pasha cells are described in more detail in previous publications [15,20]. The main feature of stencilled fingers is the higher aspect ratio compared with screen-printed fingers, which enables the use of much thinner fingers with only a small loss in fill factor [20]. The stencil process has undergone several endurance tests and its robustness has been demonstrated in an industrial run of 2000 cells [15]. Standard industrial printers can be used for the stencil process; all stencilling at ECN was done using standard Baccini printers.

In experiments 1 and 2 the total front metal coverage was reduced from 8% to 5.5%, a reduction of 2.5%. V_{oc} improved by 6mV (1%) as a result of the decrease in contact recombination. Because of reduced shading losses, I_{sc} also improved significantly, as expected, by 0.3A – equating to approximately 2.5% of the total I_{sc}. With only a small loss in *FF*, the combined experiments 1 and 2 resulted in an efficiency gain of 0.5% absolute.

The third experiment, performed on a different material, was aimed at reducing the recombination under the front contacts by applying a so-called non-contacting busbar paste [21]. Since the three busbars of the n-Pasha solar cell cover around 2.5% of the total cell area, eliminating recombination losses in this region will result in an 'effective' metal area for V_{oc} of only 3%. A gain in V_{oc} was observed similar to that when the metal coverage was reduced from 8% to 5.5%: the data for experiment 3 show an increase of 6mV or 1% relative, as can be seen in Fig. 2 (green diamonds) No significant change in I_{sc} was observed, since the total metal coverage of the cell remains the same. In addition, no significant differences in *FF* were observed, resulting in an efficiency gain of 0.15% absolute.

Diffusion and passivation

Efficiency improvements due to an improved BSF, which resulted in lower BSF doping, have also been reported in previous publications [14,15]: the results presented were typically averages over groups of 10–15 cells, with top efficiencies of up to 20%. To implement such an improved processing step in industry, the results need to be stable both within and between large batches of wafers. ECN has recently improved the front- and rear-side passivation, which has stabilized the processing in such a way that the variation in V_{oc} is drastically reduced.

The average values for V_{oc}, and the variation in the results, are shown in Fig. 3 for four different experimental groups. All the groups were processed using material from the same part of a single n-Cz ingot (with similar resistivity). Improved metallization, stencilled fingers and a non-contacting busbar on the front side were applied to all cells. The first group, with the original heavily doped BSF, yields efficiencies of around 19.4% and a V_{oc} of 640mV; the variation in V_{oc} is typically 6–7mV, equating to around 1%. The improved, more lightly doped BSF (indicated by 'BSF' on the x axis) results in a higher average V_{oc}; however, there is also an increased variation in voltage of more than 12mV. By subsequently implementing an improved rear passivation (rear pass) and front passivation (front pass), it is possible to reduce the variation from 12mV to 7mV, and even improve it further, to just 4mV. Besides there being an improvement in the stability of the processing, the average V_{oc} also increases with the improved front and rear passivation: a combined increase in V_{oc} of over 10mV (1.6%) is obtained compared with the reference.

The variation in I_{sc} increased less dramatically when the new, more lightly doped BSF was implemented. Nevertheless, it was possible to reduce the variation from 0.09A (1%) to only 0.06A by using the improved rear- and front-side passivation. Combining the more lightly doped BSF with the improved front- and rear-side passivation, a total increase of 0.1A (1.2%) was obtained compared with the reference. The resulting gain in efficiency was 0.4–0.5% absolute.

To further assess the stability of the high-efficiency processing, two large batches of wafers were processed at ECN. These batches consisted of material from two different industrial suppliers, with resistivities ranging from 3 to 5.5Ωcm for material A, and from 3 to 4.5Ωcm for material B. Both resistivity ranges were measured after a high-temperature step to annihilate the thermal donors in the material. Material A had a lower material quality, which was evident from its shorter bulk lifetime and resulting lower efficiency. The processing was carried out at ECN using industrial tools, along with the improved metallization, diffusion and passivation processes described above.

The results for both batches of wafers, including the standard deviation of the cell parameters, are shown in Table 1. For material B in particular, high efficiencies were obtained, but, more importantly, the spread in cell parameters (especially I_{sc} and V_{oc}) for both materials was very small. Average efficiencies of 19.5% (material A) and 19.7% (material B) were obtained, with top efficiencies of 19.8% and 19.9% respectively. The variation in this case is indicated by the standard deviation: for the efficiency this amounts to only 0.13% for both materials.

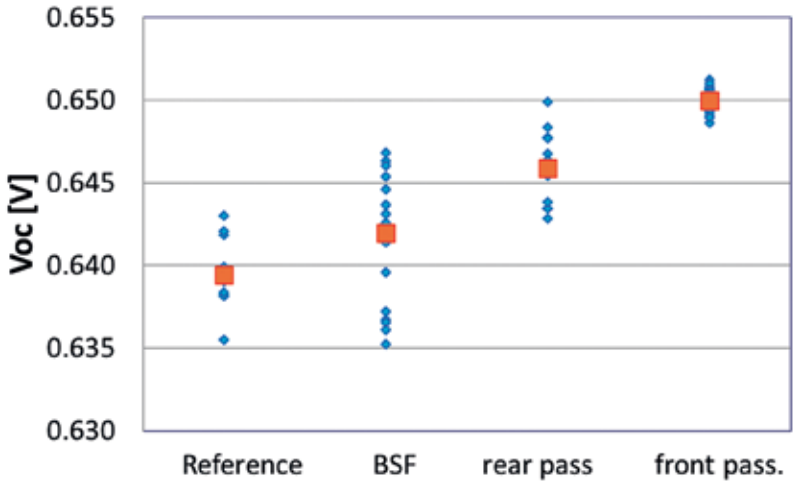

Figure 3. The increase in V_{oc} as a result of processing improvements for n-Pasha: starting from a reference 19.5% n-Pasha cell (640mV), the BSF, rear-side passivation and front-side passivation were subsequently improved. The variation in the resulting V_{oc} increased with the improved, more lightly doped BSF, but decreased for the subsequent improvements in rear- and front-side passivation.

Impact of the material

One factor that needs to be taken into account when manufacturing solar cells from n-Cz base material is the larger range of resistivity in n-Cz ingots compared with

	I_{sc} [A]	V_{oc} [V]	*FF* [%]	η [%]
Material A				
Over 252 cells	9.25	0.649	77.4	19.5
Best cell	9.30	0.652	78.7	19.8
Std dev	0.02	0.002	0.03	0.13
Material B				
Over 107 cells	9.25	0.650	78.0	19.7
Best cell	9.31	0.653	78.7	19.9
Std dev	0.02	0.002	0.04	0.13

Table 1. Results for the processing of large batches of materials.

that in p-type ingots [16]. This difference is due to the high segregation coefficient of phosphorus in the Cz crystal growth process. Typical resistivity ranges for n-Cz material are 0.5–2Ωcm at the tail and reaching up to 8–10Ωcm (or even up to 12Ωcm) at the seed of the ingot. The base resistivity variation will influence the cell parameters: higher values of I_{sc} and lower *FF*s are predicted for higher base resistivities [18].

To check the dependency of ECN n-Pasha cell performances on base resistivity, cells were fabricated from n-Cz material taken from different parts of a single ingot; the base resistivity varied between 2.5 and 10Ωcm. For these experiments n-Pasha cells were made using both the original, heavily doped BSF and the improved, lightly doped BSF with the improved front and rear passivation. Every cell had the improved metallization on the front side. The *I-V* results shown in Fig. 4 represent the average values of approximately five cells per group.

> "One factor that needs to be taken into account when manufacturing solar cells from n-Cz base material is the larger range of resistivity in n-Cz ingots compared with that in p-type ingots."

The results for V_{oc} and I_{sc} are shown in Figs. 4(a) and 4(b): the higher values of I_{sc} and V_{oc} along the complete resistivity range are clearly visible for the lightly doped BSF as compared to the heavily doped BSF. As expected, the value of I_{sc} increases with higher base resistivity (and thus lower base doping) because of the lower recombination losses. At the same time, the value of V_{oc} shows only a very slight decrease with increasing base resistivity [22].

The values for V_{oc} and I_{sc} have been fitted using PC1D. The front-side parameters (S_{front}, emitter profile) have been kept constant, using a p^+ emitter with an R_{sheet} of 61Ω/sq. The same, high bulk lifetime has been assumed for all cases, while the base resistivity R_{base} has been changed. Compared with cells with the heavily doped BSF, cells with the more lightly doped BSF were fitted with less free-carrier absorption (represented by a higher internal reflection in the PC1D model), better passivation (lower S_{rear}) and lighter doping (higher R_{BSF}). As can be seen in Figs. 4(a) and 4(b), V_{oc} and I_{sc} can be fitted quite well within the measurement error.

The *FF* and efficiency values are shown in Figs. 4(c) and 4(d). The *FF* indeed decreases with higher base resistivity. However, the drop in *FF* is counteracted by the increase in I_{sc}, which results in a stable and high average efficiency of 19.8% between 2 and 10Ωcm for the lightly doped BSF case, and a stable efficiency of 19.4% between 2 and 10Ωcm for the heavily doped BSF case.

There is still room for improvement of the *FF* in the lightly doped BSF case: for all cells, with both lightly and heavily doped

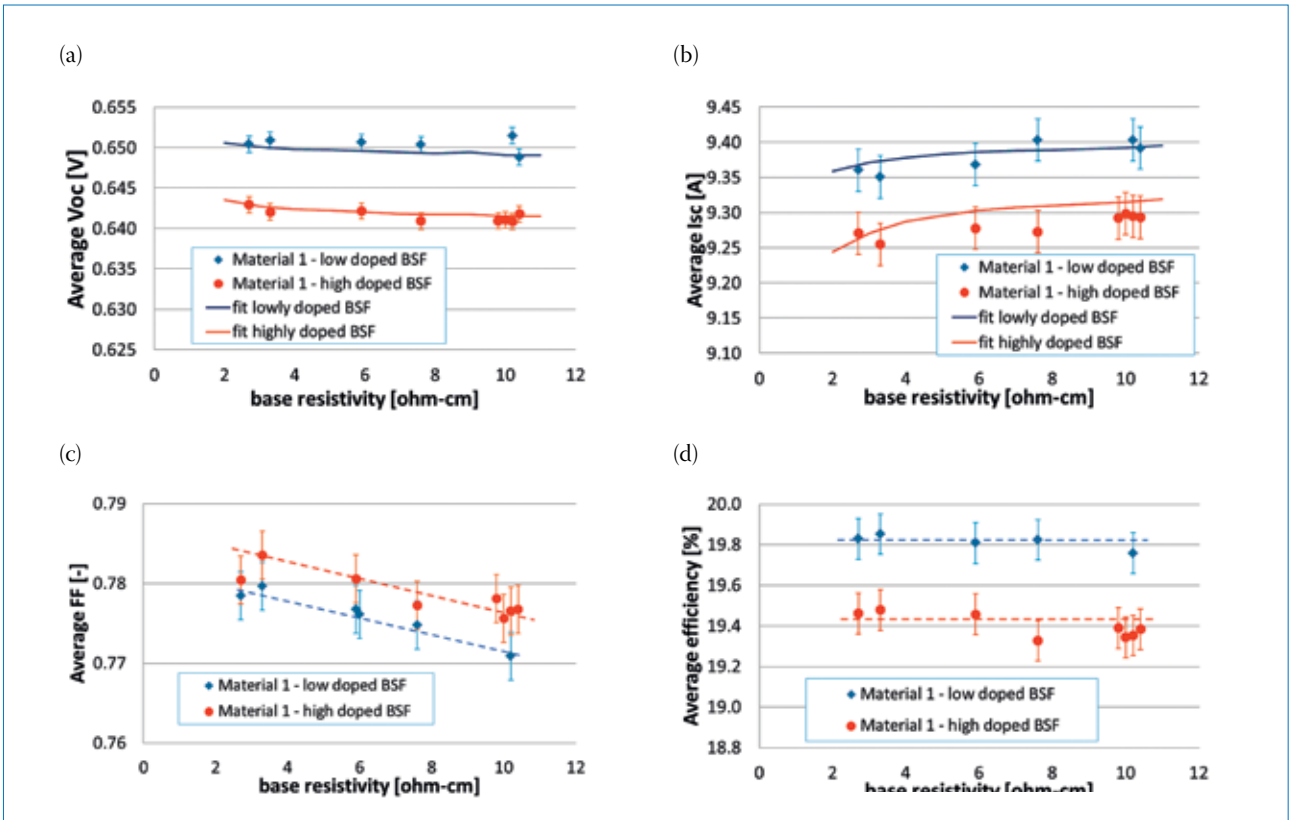

Figure 4. *I-V* results for n-Pasha cells made using both the original, heavily doped BSF and the improved, lightly doped BSF with the improved front and rear passivation: (a) V_{oc}; (b) I_{sc}; (c) *FF*; (d) η.

BSFs, the rear-side metallization pattern used was identical and optimized for the heavily doped BSF conductivity. On the basis of simulations it is expected that the *FF* for the more lightly doped BSF cells can be made comparable to that for the heavily doped BSF cells by optimizing the rear metallization pattern. Modelling indicates that the implementation of an improved rear metal-grid design with more, but smaller, fingers will increase the efficiency of the lightly doped BSF to an average of 20% for a base resistivity range of 2–10Ωcm.

Besides the dependency of the n-Pasha cell processing on base doping, n-Pasha cell processing using material from several different suppliers has been investigated. Material from eight different commercial suppliers was used for this investigation. The base resistivities of the materials varied between 2 and 10Ωcm. In this experiment, the efficiency of the n-Pasha cells depends on the material quality, or on the bulk lifetime, of the different wafers. Fig. 5 shows the average efficiency values for n-Pasha cells made with the high-efficiency processing using the eight materials. For materials 1, 3 and 6–8, average efficiencies of 19.8% were obtained. Materials 4 and 5 fared better, demonstrating average efficiencies of 19.9% and 20%. The best efficiency of 20.2% was achieved with material 2 (in-house measurement using a reflecting measurement chuck to simulate the situation in a module, and reference cells calibrated at ISE Cal lab). The average and best cell results for material 2 are summarized in Table 2.

These results show that the n-Pasha cell concept makes it possible to obtain high efficiencies using n-Cz material having a large variation in resistivity, and also using material from many commercial wafer manufacturers. This proves that the n-Pasha cell concept is an excellent route to creating high-efficiency industrial solar cells from n-type base material.

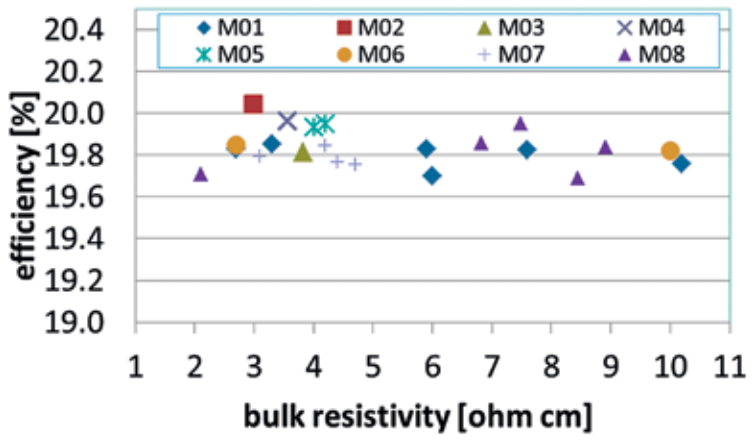

Figure 5. Average efficiencies for n-Pasha cells (with lightly doped BSF) fabricated using material from eight different commercial wafer suppliers.

	I_{sc} [A]	J_{sc} [mA/cm^2]	V_{oc} [V]	*FF* [%]	η [%]
Average	9.38	39.23	0.652	78.3	20.04
Best cell	9.40	39.33	0.653	78.8	20.23

Table 2. Average and best cell *I-V* characteristics for material 2.

Cost reduction

Reducing Ag consumption has been a driving force in improving the cost effectiveness of n-Pasha solar cells. Fig. 6 shows the silver consumption on the front and rear sides of n-Pasha cells for 2012 and 2013, relative to the consumption in 2011; the average consumption for a conventional p-type solar cell is also shown. To make a fair comparison, the costs of the aluminium consumption for the p-type cells have been recalculated in terms of the equivalent milligrams of silver for the rear side, since the aluminium is absent in the case of n-Pasha cells.

For the front side of an n-Pasha cell, the silver consumption has been reduced by almost 40% relative in 2012 by: 1) adopting a stencil print [14,15], which allows thinner fingers without a loss in fill factor; and 2) replacing the standard busbar paste by the non-contacting busbar paste [21], which also has a lower silver content. Both changes have contributed to an efficiency gain of around 0.5% absolute as described above. The front-side silver consumption for an n-Pasha cell is now already less than the average consumption for the front-side of a conventional p-type cell.

For the rear side, the silver reduction that was realized in 2012 is even more extreme. Thinner fingers, and again an improved silver paste [23], have enabled a silver reduction of almost 70% without any loss in efficiency. ECN's goal for 2013 is to decrease the Ag consumption even further, to just 50% of the original consumption on the front and to just 25% on the rear, by further paste and pattern optimizations.

For solar cell manufacturers, the total silver consumption per output power (Wp) is very important for their cost of ownership calculations. This parameter can be seen in Fig. 7. The first two bars show the total silver consumption for n-Pasha cells made in 2011, with 19% average efficiency, and for n-Pasha cells made in 2012, with 20% average efficiency. In 2013, the silver consumption will be reduced further, as shown in Fig. 6; the aim is also, of course, to improve the efficiency to a value of 21%. The silver consumption target in 2013 is therefore calculated for both 20% and 21% efficiencies. The last bar on the chart shows the silver consumption for a typical p-type Cz solar cell with an average efficiency of 18.5%. The figures show that the silver consumption per Wp in 2012 for n-Pasha cells was comparable

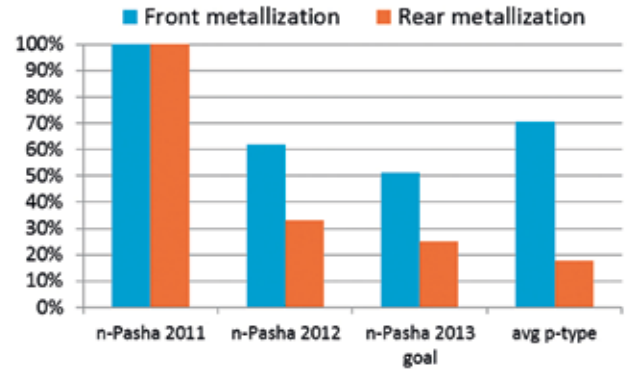

Figure 6. Relative Ag reduction for front and rear metallization of n-Pasha cells, and a comparison with the average Ag usage for p-type cells.

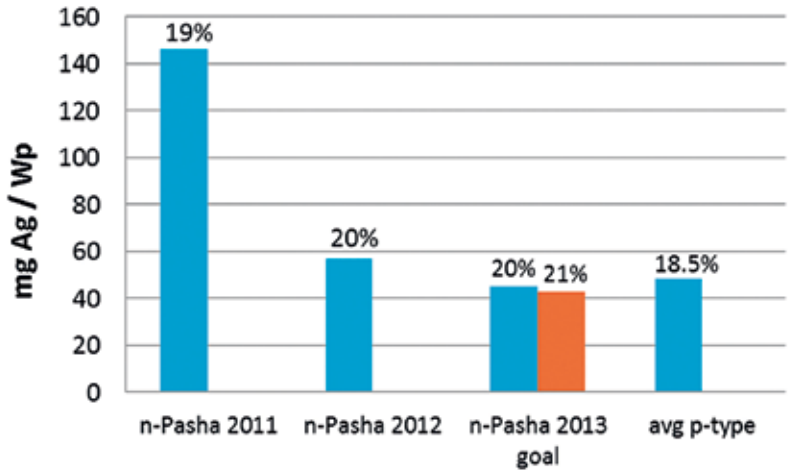

Figure 7. Silver consumption per cell per output power (Wp) for n-Pasha cells in 2011–2013, compared with p-type cells with average 18.5% efficiency.

to that for p-type cells, but is expected to be lower in 2013.

"Silver consumption per Wp in 2012 for n-Pasha cells was comparable to that for p-type cells, but is expected to be lower in 2013."

Further developments in 2013 and beyond

The next steps to improve the n-Pasha cell concept even further will be to increase the cell efficiency to 21% and decrease the processing costs at the same time. The topics for development will be:

1. Further reduction of the silver consumption of the printed metallization, especially on the rear side, by printing and pattern optimizations.

2. Optimization of the emitter profile and front-surface passivation. Thanks to the improved rear diffusion, front-surface passivation and reduced front-side metallization, improvements will become more beneficial.

3. Reduction of the front-metal silver consumption, and at the same time improvements in I_{sc} and V_{oc} without a loss in *FF*, by introducing a metal wrap-through (MWT) cell concept [24,25]. An additional advantage of this MWT cell concept is the lower series resistance interconnection losses when the cells are interconnected to make up a module, which results in an improved cell-to-module ratio [26].

4. Further reductions in silver consumption by using only local Ag contacts on the rear side and connecting these by a full-area deposited layer of cheaper metal, such as aluminium. With this so-called PERT structure, higher values of I_{sc} and V_{oc} are expected as well.

Conclusions

The n-Pasha solar cell concept has been optimized in terms of both efficiency and cost. Improvements in front-side metallization, depending on the technology used (stencil vs. screen print) and the type of paste, resulted in a stable improvement in V_{oc} of ~10mV, an improvement in I_{sc} of 0.3A and a gain in efficiency of 0.5% absolute because of the reduction in metal coverage and contact recombination. Moreover, an optimized BSF diffusion in combination with front and rear passivation resulted in another stable improvement in V_{oc} of ~10mV and a 20% average efficiency, with 20.23% being achieved for the best cell.

"The combination of efficiency improvement and cost reduction makes the n-Pasha cell concept a very cost-effective solution for manufacturing highly efficient solar cells and modules."

Stability of the process has been demonstrated for several large batches with >100 and >230 cells, and using n-Cz material of various qualities and from different suppliers. Special attention was given to the solar cell dependence on the base resistivity of the n-Cz material, which is also one of the major challenges for n-Cz. The high-efficiency n-Pasha process is stable in a wide resistivity range of 2–10Ωcm, and optimization steps have been identified, for example the use of a dedicated rear-contact pattern or *FF* optimization.

Significant steps have been taken with regard to silver reduction for both the front and the rear metallization of n-Pasha cells: the total silver consumption is now comparable to that of conventional p-type cells. The combination of efficiency improvement and cost reduction makes the n-Pasha cell concept a very cost-effective solution for manufacturing highly efficient solar cells and modules.

Acknowledgements

The authors would like to thank Yingli Solar, Tempress Systems BV, RENA GmbH, Heraeus GmbH and Merck KGaA for their fruitful cooperation in improving the n-Pasha cell concept. Special thanks to M. Koenig for the expeditious development of new silver pastes for n-Pasha cells.

References

[1] SEMI PV Group Europe 2013, "International technology roadmap for photovoltaic (ITRVP): Results 2012", 4th edn (March) [available online at http://www.itrpv.net/Reports/Downloads/].

[2] Schmidt, J. et al. 1997, *Proc. 26th IEEE PVSC*, Anaheim, California, USA, p. 13.

[3] Glunz, S. et al. 1998, *Proc. 2nd WCPEC*, Vienna, Austria, p. 1343.

[4] Macdonald, D. & Geerligs, L.J. 2008, *Appl. Phys. Lett.*, Vol. 92, p. 4061.

[5] Cotter, J.E. et al. 2005, *Proc. 15th Worksh. Cryst. Si. Sol. Cells & Mod.: Mater. & Proc.*, p. 3.

[6] SunPower [details online at http://us.sunpowercorp.com/about/sunpower-technology/most-efficient-solar/].

[7] Cousins, P. et al. 2010, *Proc. 35th IEEE PVSC*, Honolulu, Hawaii, USA.

[8] SNE Research 2011, "Next-generation high efficiency crystalline Si solar cell technology and market forecast (2008–2015)" [details online at http://www.researchandmarkets.com/reports/2082445/nextgeneration_high_efficiency_crystalline_si].

[9] Mishima, T. et al. 2011, *Solar Energy Mater. & Solar Cells*, Vol. 95, pp. 18–21.

[10] Panasonic [details online at http://eu-solar.panasonic.net/en/products/n-240-n-235].

[11] Geerligs, L.J., Guillevin, N. & Romijn, I.G. 2011, *Photovoltaics International*, 12th edn, p. 94.

[12] Burgers, A.R. et al. 2011, *Proc. 26th EU PVSEC*, Hamburg, Germany.

[13] Song, D. et al. 2012, *Proc. 38th IEEE PVSC*, Austin, Texas, USA.

[14] Romijn, I.G. et al. 2012, *Proc. 27th EU PVSEC*, Frankfurt, Germany.
[15] Romijn, I.G., Fang, L. & Vlooswijk, A. 2012, *Photovoltaics International*, 15th edn, p. 81.
[16] Kopocek, R. & Libal, J. 2012, "Switch from p to n", *PV Magazine*.
[17] Komatsu, Y. et al. 2009, *Solar Energy Mater. & Solar Cells*, Vol. 93, pp. 750–752.
[18] Boescke, T.S. et al. 2012, *Proc. 38th IEEE PVSC*, Austin, Texas, USA.
[19] Fellmeth, T. et al. 2011, *Energy Procedia*, Vol. 8, pp. 115–121.
[20] Heurtault, B. & Hoonstra, J. 2010, *Proc. 25th EU PVSEC*, Valencia, Spain.
[21] Koenig, M. et al. 2012, *Proc. 2nd Silicon PV*, Leuven, Belgium.
[22] Green, M.A. 1998, *Solar Cells, Operating Principles, Technology and System Applications*, Kensington, Australia: University of New South Wales.
[23] Karpowich, L. et al. 2012, *Proc. 27th EU PVSEC*, Frankfurt, Germany, pp. 1766–1768.
[24] Guillevin, N. et al. 2012, *Proc. 27th EU PVSEC*, Frankfurt, Germany.
[25] Zhao, W. et al. 2012, *Proc. 27th EU PVSEC*, Frankfurt, Germany.
[26] Tool, C.J.J. et al. 2012, *Proc. PVSEC 22*, Hangzhou, China.

About the Authors

Ingrid Romijn joined ECN Solar Energy in 2004, where she started working as a researcher and then later on as a project leader (2006) in the crystalline silicon group. Research topics included passivation layers, optimization of SiN_x deposition systems and (advanced) p-type solar cell concepts. During 2011 the focus of her work shifted towards the development and industrialization of n-type cell concepts. In 2012 Ingrid became the topic coordinator for industrial n-type cells and modules at ECN Solar Energy.

Astrid Gutjahr studied mineralogy at the University of Bonn in Germany and was a postdoctoral researcher in the Liquid Phase Epitaxy group at the Max Planck Institute for Solid State Research in Stuttgart. In 1999 she joined ECN, where she has worked on the development of RGS, a crystalline Si ribbon growth technology. Astrid's current research focuses on characterization and cell processing of n-type silicon wafer material.

Desislava Saynova joined ECN in 2007, where she has been working on various projects in the field of characterization and design optimization of high-performance solar cells based on both p- and n-type c-Si. Desislava has also been involved in the investigation of different silicon materials, such as ribbons and compensated ingots, for optimizing performance in PV applications. Since 2010 one of her major research tasks has been the development of n-type solar cell concepts for industrial applications.

Kees Tool has worked in the solar energy field for almost 20 years. After receiving his education in chemistry, he began his solar energy career as a researcher. Over the last seven years, his main work has involved the transfer of ECN n-type and p-type technology to industry. Kees also performs troubleshooting and tuning of industrial crystalline silicon solar cell production lines, as well as being responsible for the quality of the ECN p-Cz base process.

Enquiries

ECN Solar Energy
P.O. Box 1
NL-1755 ZG Petten
The Netherlands

Tel: +31 224 56 4959
Fax: +31 224 56 8214
Email: romijn@ecn.nl